A Miniaturized System for Spike-Triggered Intracortical Microstimulation in an Ambulatory Rat

Meysam Azin, *Student Member, IEEE*, David J. Guggenmos, Scott Barbay, Randolph J. Nudo, and Pedram Mohseni*, *Senior Member, IEEE*

***Abstract*—This paper reports on a miniaturized system for spike-triggered intracortical microstimulation (ICMS) in an ambulatory rat. The head-mounted microdevice comprises a previously developed application-specific integrated circuit fabricated in 0.35-μm two-poly four-metal complementary metal–oxide–semiconductor technology, which is assembled and packaged on a miniature rigid-flex substrate together with a few external components for programming, supply regulation, and wireless operation. The microdevice operates autonomously from a single 1.55-V battery, measures 3.6 cm $\times$ 1.3 cm $\times$ 0.6 cm, weighs 1.7 g (including the battery), and is capable of stimulating as well as recording the neural response to ICMS in biological experiments with anesthetized laboratory rats. Moreover, it has been interfaced with silicon microelectrodes chronically implanted in the cerebral cortex of an ambulatory rat and successfully delivers electrical stimuli to the second somatosensory area when triggered by neural activity from the rostral forelimb area with a user-adjustable spike-stimulus time delay. The spike-triggered ICMS is further shown to modulate the neuronal firing rate, indicating that it is physiologically effective.**

***Index Terms*—Activity-dependent microstimulation, ambulatory rat, intracortical microstimulation (ICMS), miniaturized system, neural recording, spike discrimination, spike-triggered neurostimulation, system-on-chip.**

I. Introduction

TO DATE, brain–machine interfaces (BMIs) have sought to interface the brain with the external world using intrinsic neuronal signals as input commands for controlling external devices [1]–[3], or device-generated electrical signals to mimic sensory inputs to the nervous system [4], [5]. A new generation of neuroprostheses is now emerging that aims to combine neural recording, neural signal processing, and microstimulation functionalities in a single device, creating an artificial connection in the nervous system by converting neural activity recorded from one cortical area to electrical stimuli delivered to another cortical area [6], spinal cord [7], or muscles [8] in real time.

Such activity-dependent neural stimulation is shown to induce neuronal plasticity for functional reorganization in an intact nervous system [9], and is envisioned to have numerous applications such as restoring function after neuronal injury [8], providing refined sensory inputs in neuroprosthetic systems [10] or supporting closed-loop therapeutic interventions for neuropathologies [11], [12].

One of the first examples of such engineered devices is reported by Fetz and colleagues, which incorporates a recording and digitization front-end, programmable microcontroller for real-time spike discrimination, biphasic constant-current microstimulator, nonvolatile memory to store biological data, and an infrared data link for wireless communication with a PC [6]. The device is built with commercial off-the-shelf (COTS) components on a custom printed-circuit board (PCB) that measures 1.2 cm $\times$ 5.4 cm, weighs 26 g (including a 3.3-V lithium battery), and is enclosed in a 5.5 cm $\times$ 5 cm $\times$ 3 cm titanium case with a lid that is mounted on a monkey's head and weighs an additional 30 g. In experiments with awake, freely behaving monkeys, the device can successfully deliver stimuli to one electrode triggered by neural spikes recorded at a separate site (1–2 mm away), inducing conditioning effects in an intact nervous system that is dependent on the relative timing of spikes and stimulus [9].

More recently, Carmena and colleagues have reported a low-cost system using COTS components, custom PCBs and software that can be interfaced with standard commercially available electrophysiology equipment for neural recording and closed-loop intracortical microstimulation (ICMS) in awake, freely behaving rats [10]. The system is capable of recording and microstimulation through the same chronically implanted microwire array as well as triggering ICMS in response to action potentials, features in the local field potentials (LFP), or behavioral events such as whisking. The system is envisioned to have applications in closed-loop neuroprostheses by providing refined sensory feedback information to the user.

There are emerging applications for activity-dependent ICMS as well. Researchers have recently demonstrated the remarkable ability of cortical areas remote from an infarct to form new

Manuscript received January 5, 2011; revised March 12, 2011 and May 12, 2011; accepted June 8, 2011. Date of publication June 16, 2011; date of current version August 19, 2011. This work was supported by the Department of Defense (DOD) Traumatic Brain Injury-Concept Award Program under Award W81XWH-08-1-0168, DOD Traumatic Brain Injury-Investigator-Initiated Research Award Program under Award W81XWH-10-1-0741/0742, and the American Heart Association under Award 09BGIA2280495. The chip fabrication costs were generously supported by the Advanced Platform Technology (APT) Center—A Veterans Affairs (VA) Research Center of Excellence, Cleveland, OH. *Asterisk indicates corresponding author.*

M. Azin was with the Department of Electrical Engineering and Computer Science, Case Western Reserve University, Cleveland, OH 44106 USA. He is now with the West Wireless Health Institute, La Jolla, CA 92037 USA (e-mail: mxa208@cwru.edu).

D. J. Guggenmos, S. Barbay, and R. J. Nudo are with the Department of Molecular and Integrative Physiology and the Landon Center on Aging, University of Kansas Medical Center, Kansas City, KS 66160 USA (e-mail: dguggenmos@kumc.edu; SBARBAY@kumc.edu; rnudo@kumc.edu).

*P. Mohseni is with the Department of Electrical Engineering and Computer Science, Case Western Reserve University, Cleveland, OH 44106 USA (e-mail: pedram.mohseni@case.edu).

Color versions of one or more of the figures in this paper are available online at http://ieeexplore.ieee.org.

Digital Object Identifier 10.1109/TBME.2011.2159603

axonal connections *spontaneously* over long distances between the frontal and parietal lobes in nonhuman primates [13]. While chemical cues may guide growth during development and after injury, activity-dependent ICMS might be able to provide the electrical signal to guide postinjury axonal sprouting and repair interrupted cortical pathways directly in the brain by driving temporal coupling of activity between brain regions [14]. Such guided repair strategies might aid in functional recovery after brain injury and are in contrast to more traditional BMI approaches that aim to replace the lost pathways.

We have previously developed a custom, application-specific integrated circuit (ASIC) for multichannel spike-triggered ICMS [15]. The system and transistor-level circuit architectures as well as performance characterization during electrical benchtop measurements and biological experiments with anesthetized rats were thoroughly described in [15].

In this paper, we present a miniaturized, head-mounted microdevice for spike-triggered ICMS created by custom assembly and packaging of the ASIC on a rigid-flex substrate. The microdevice is the smallest, most lightweight system yet developed for use with an ambulatory rat and is capable of stimulating and recording the neural response to ICMS as well as performing spike-triggered ICMS with user-adjustable spike-stimulus time delay. In the long term, this miniaturized system is envisioned to be used with a rat model of injury and recovery [16] to investigate the feasibility of reshaping intracortical connectivity patterns after traumatic brain injury (TBI) using spike-triggered ICMS.

This paper is organized as follows. Section II presents the experimental setup and describes its individual components in further detail. Section III presents the biological results from experiments with anesthetized and ambulatory rats. Finally, Section IV draws some conclusions from this study.

II. Spike-Triggered ICMS

Fig. 1 shows an illustration of our experimental setup for spike-triggered ICMS in an ambulatory rat. The previously developed ASIC together with a minimum number of external components and a single coin battery (1.55 V) are assembled on a rigid-flex substrate to create a miniature, head-mounted microdevice. Neural data can be transmitted wirelessly via a radio-frequency frequency-shift-keyed (RF-FSK) link at ∼433 MHz between the microdevice and a commercial RF receiver (AOR, Torrance, CA), which downconverts the RF signal to an intermediate frequency (IF) of 10.7 MHz. A wired connection can be temporarily attached to the microdevice for programming and monitoring its operation status. A custom external receiver board is used for signal conditioning and decoding of wired and wireless signals. A digital data acquisition (DAQ) card (National Instruments, Austin, TX) establishes a high-speed connection between the receiver board and a PC used for microdevice programming as well as storage and analysis of the recorded data with MATLAB.

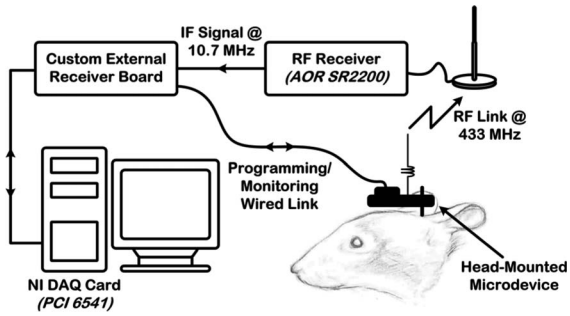

Fig. 1. Experimental setup, depicting a head-mounted microdevice for spike-triggered ICMS in an ambulatory rat and peripheral devices for programming and monitoring.

A. ASIC Overview

In this section, we present the architecture and measured performance metrics of the 3.3 mm × 3.3 mm ASIC for spike-triggered ICMS, which is previously developed in a 0.35-μm two-poly four-metal (2P/4M) complementary metal–oxide–semiconductor (CMOS) technology [15]. Fig. 2 depicts the block diagram and a die micrograph of the chip. Each four-channel module of the chip incorporates a recording front-end, a digital signal processing (DSP) unit, and a stimulating back-end. For autonomous operation from a single 1.55-V battery, the ASIC also integrates a dc–dc converter that generates 5 V from the battery as the power supply for the stimulating back-end. It is capable of delivering ICMS sequences via an external trigger as well as triggered by neural spikes discriminated in real time, with precise control over the stimulation time instance.

The recording front-end features a bandpass frequency response with the low and high cutoff frequencies programmable from 1.1 to 525 Hz and 5.1 to 12 kHz, respectively, and provides 2b-programmable ac amplification (nominal gain of ∼60 dB at 1 kHz), dc input stabilization, and 10b digitization of the recorded neural signals.

The DSP unit in each module provides additional digital high-pass filtering to remove any residual dc offsets or low-frequency artifacts and subsequently performs real-time spike discrimination based on threshold crossing and two user-adjustable time-amplitude windows. The digital high-pass filter (HPF) in the DSP unit has a programmable cutoff frequency of 366 or 756 Hz, given a 1-MHz system clock. If a spike event is accepted on any channel, the corresponding spike discriminator output (SDO) is activated after a programmable time delay (0 to ∼28.6 ms).

The decision circuitry then generates any logic combination of SDO 1∼4 as a trigger signal for stimulation activation. Upon triggering, the programmable stimulating back-end delivers a charge-balanced asymmetric biphasic stimulus or monophasic stimulus with passive discharge to the neural tissue. The anodic and cathodic current pulse amplitudes are 6b-programmable from 0 to 94.5 μA and 31.5 μA, respectively. With a 1-MHz system clock, the duration of the anodic phase can be programmed from 0 to 240 μs with a resolution of 16 μs, whereas that of the cathodic phase is programmable from 0 to 720 μs with a resolution of 1 μs. For monophasic stimulation, the duration of the constant-current phase is programmable from 0 to 1.008 ms

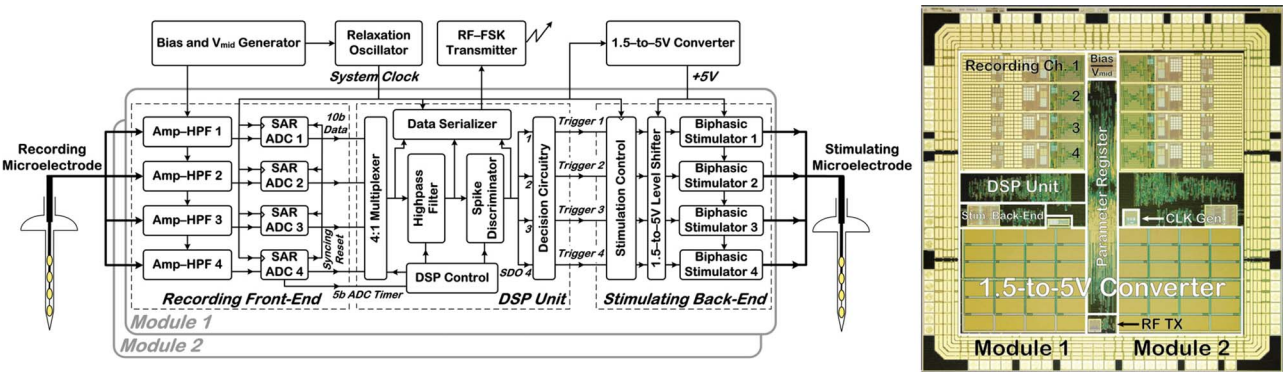

Fig. 2. Block diagram and a die micrograph of the 3.3 mm × 3.3 mm ASIC for spike-triggered ICMS. There are two identical four-channel modules per chip powered by a single 1.55-V battery. The chip is fabricated in a 0.35-μm 2P/4M CMOS technology [15].

with a resolution of 16 μs. Passive discharge is performed after *each* constant-current phase to drain the accumulated charge on the stimulation site via a 2b-programmable resistor.

In constructing the head-mounted microdevice and for all biological experiments described next, one four-channel module of the ASIC is used for spike-triggered ICMS. Further, in the nominal operating condition of the ASIC, the bandwidth of the recording front-end is set to be 525 to 5.1 kHz and the cutoff frequency of the digital HPF is set to 366 Hz. The stimulating back-end is also programmed to deliver a single monophasic current pulse (duration of 192 μs) with variable amplitude followed by passive discharge, upon receiving an external or neural-based stimulus trigger.

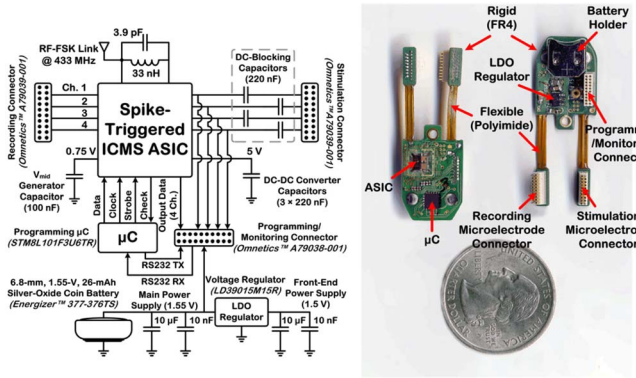

Fig. 3. Block diagram and a photograph of the fully assembled microdevice. The prototype device currently uses one four-channel module of the ASIC for spike-triggered ICMS in an ambulatory rat.

B. Microdevice Architecture

Fig. 3 shows the block diagram and a photograph of the assembled microdevice for use with an ambulatory rat. Various components are assembled on a four-layer rigid-flex PCB made from FR-4 and polyimide (Flexible Circuit Technologies, Plymouth, MN). The microdevice connects to two chronically implanted recording and stimulation microelectrodes via two microconnectors (Omnetics Corporation, Minneapolis, MN) in plug-and-play fashion. The microelectrodes are not permanently connected to the microdevice in order to allow replacing the microdevice in case of failure or for reuse in additional experiments. The flexible polyimide interconnect between the microelectrode connectors and the rigid substrate allows for some adjustability in microelectrode placement during implantation, simplifying the surgical procedure. For safe operation, four dc-blocking capacitors (220 nF) are placed in series with the stimulation channels to prevent any net dc current flow into the tissue, potentially arising from semiconductor failure or charge imbalance. A 6.8-mm, 1.55-V, silver-oxide, coin battery with capacity of 26 mAh (Energizer, St. Louis, MO) is selected to power the microdevice due to its small size and stable output voltage. The onboard battery powers the device continuously at its nominal operating condition for 24 h.

A low-power, low-voltage, commercial microcontroller (ST Microelectronics, Geneva, Switzerland) programs the ASIC during power-up and then shuts down to reduce the static power consumption. The ASIC checks the validity of the programming parameters using two 10b redundant codes. If both codes in the parameter data stream are equal to those hardwired inside the chip, the *Check* signal is activated; otherwise, the ASIC sends an interrupt signal to the microcontroller to turn it back on for reprogramming. A new parameter data stream can be sent to the microcontroller from the PC via the external receiver board using a bidirectional RS232 asynchronous serial link. The data are saved inside the microcontroller EEPROM and then shifted into the chip. Once ASIC programming is successful, the microcontroller transmits an acknowledgment signal back to the PC.

The FSK wireless link in the microdevice can transmit either the full-voltage record on one channel or spike discrimination events on all four channels to the RF receiver placed as far as 2 m from the rat. A 5-cm twisted wire is used as the antenna connected to one side of an external resonant inductor (33 nH)–capacitor (3.9 pF) *LC* tank. These *LC* components result in an RF link frequency of ∼433 MHz, given a tolerance of 5% in their values and parasitic contribution by input–output (I/O) pads, wire bonds, and PCB interconnects. The wireless recording of broad-band neural data is currently limited to a single channel due to battery lifetime considerations for supporting higher data rates. Nonetheless, the raw data recorded on all four channels of the microdevice can still be accessed simultaneously using a wired link between the microdevice and the external receiver

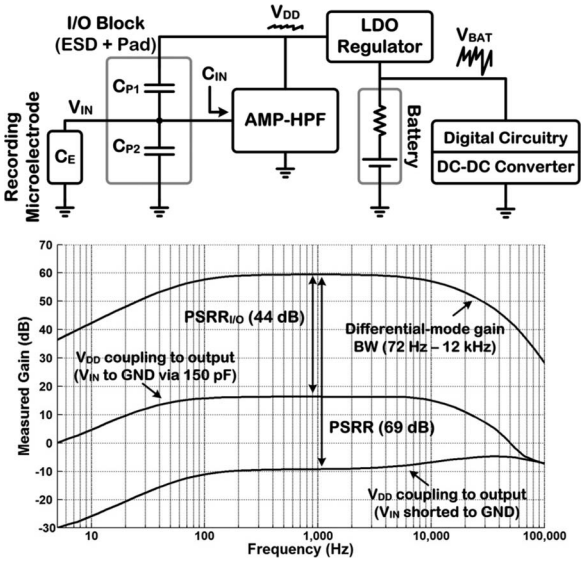

Fig. 4. Mechanism for PSRR degradation in the analog recording front-end when interfaced with a recording microelectrode. (Top) Block diagram. (Bottom) Measured PSRR with the input hardwired to ground as well as grounded via a 150-pF external capacitor.

board. The wired connection also provides the output voltage level on all four stimulation channels to monitor stimulation site impedance during long-term experiments.

A commercial low-dropout (LDO) voltage regulator (ST Microelectronics, Geneva, Switzerland) together with four external capacitors are used to isolate the power supply line of the sensitive front-end recording circuitry from that of the rest of the system, mainly the noisy digital circuitry and 1.5-to-5 V converter. Given the nonzero source impedance of the silver-oxide coin battery (5 to 10 Ω), this scheme is critical to ensure robust, reliable operation of the sensitive recording front-end. Although the power supply rejection ratio (PSRR) of the recording front-end is measured to be >65 dB [15], this measurement is typically done with the input shorted to ground. As depicted schematically in Fig. 4, the combination of the recording microelectrode capacitance C_E and parasitic capacitors $C_{P1,2}$ in the analog I/O block contributed by electrostatic discharge protection circuitry and bonding pad creates an additional signal path for the supply induced noise that can degrade the PSRR in practice. From Fig. 4, the PSRR through I/O parasitic capacitors can be derived as

$$\mathrm{PSRR_{I/O}} = \frac{C_E + C_{p1} + C_{p2} + C_{\mathrm{IN}}}{C_{P1}} \cong \frac{C_{\mathrm{IN}} + C_E}{C_{P1}} \quad (1)$$

where C_{IN} is the input capacitance of the recording front-end, which is 28 pF in this study. Given C_E of 150 pF (i.e., recording site impedance of ∼1.1 MΩ at 1 kHz) and estimated values of 1 pF for $C_{P1,2}$, (1) results in $\mathrm{PSRR_{I/O}}$ of 45 dB. Fig. 4 also shows the measured PSRR with V_{IN} shorted to ground as well as that with V_{IN} connected to ground via a 150-pF external capacitor. $\mathrm{PSRR_{I/O}}$ was measured to be ∼44 dB at 1 kHz, in good agreement with (1). Therefore, measured noise of 10 $\mathrm{mV_{pp}}$ on the battery voltage would induce ∼63-$\mu\mathrm{V_{pp}}$ noise on the input, greatly degrading the recording signal-to-noise ratio. Instead, the LDO regulator attenuates the power supply noise by more than 60 dB at 1 kHz, reducing the noise induced on the input well below the thermal and flicker noise levels of the recording front-end.

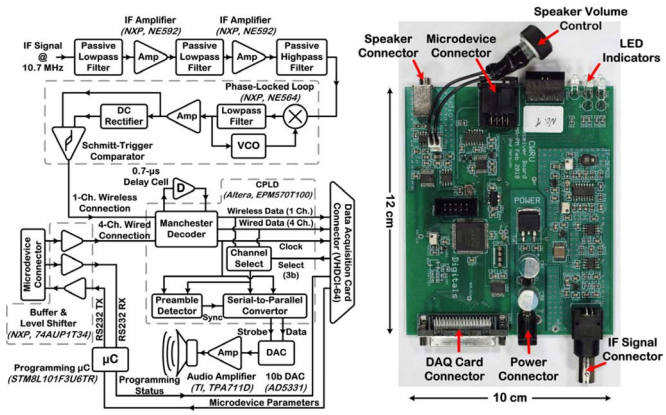

Fig. 5. Block diagram and a photograph of the external receiver board.

C. External Receiver Board

Fig. 5 shows the block diagram and a photograph of the custom external receiver board. It incorporates FSK demodulation circuitry using a commercial phase-locked loop device (NXP Semiconductors, The Netherlands), which detects the frequency variation of the amplified/filtered 10.7-MHz IF signal for further downconversion to baseband. The wirelessly received data together with four channels of wired data are processed in a complex programmable logic device (Altera, San Jose, CA), which uses a Manchester decoder for clock/data recovery and sends the signals to the PC via the DAQ card. Any one of the five data channels can be selected by the user for broadcasting of the data stream through a speaker. Specifically, a preamble detector and a deserializer unit convert the selected data stream to 10b digital codes that are then converted to an analog audio signal using a digital-to-analog converter (Analog Devices, Norwood, MA). This feature allows a trained user to rapidly identify whether neural activity is present in the recorded data stream by listening to the sound of spiking neurons. The onboard microcontroller unit receives parameter data for microdevice operation from the PC and sends them to the microdevice via a RS232 asynchronous serial link. As stated previously, if ASIC programming is successful, the microcontroller receives an acknowledgment signal from the microdevice and then sends the programming status back to the PC.

III. Biological Results

This section presents the experimental results from biological tests with anesthetized and ambulatory rats. The experiments were conducted in the cerebral cortex of adult Long-Evans rats in accordance with guidelines approved by the Institutional Animal Care and Use Committee, Kansas University Medical Center, Kansas City.

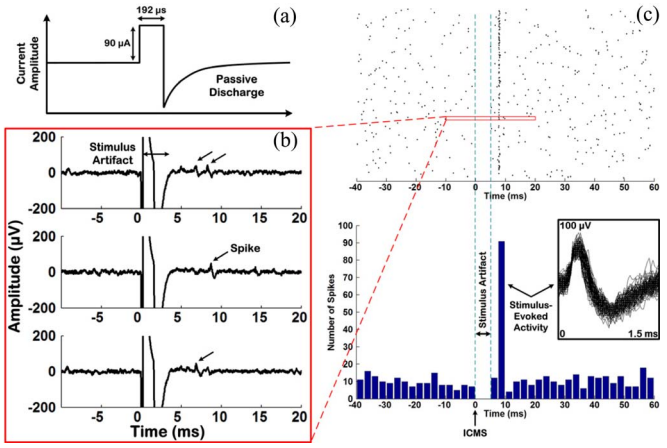

Fig. 6. Neural response to ICMS. (a) Monophasic current pulse with passive discharge delivered to the CFA of a rat's brain at 2 Hz. (b) Traces showing the neural response to ICMS. Arrows indicate spikes detected by the ASIC. (c) Rastor plot and peristimulus histogram (2.5-ms bins) of the neural response to ICMS, showing an increase in neural activity after stimulation.

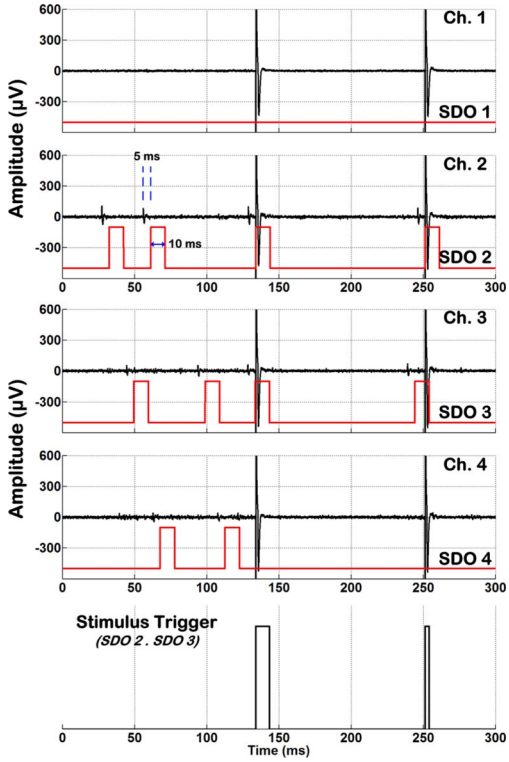

Fig. 7. Stimulation on the microelectrode implanted in the CFA triggered by neural spikes discriminated on multiple recording sites of the microelectrode implanted in the RFA. The ASIC was programmed to trigger ICMS when neural activity was discriminated on channels 2 and 3 within a 10-ms window, with the stimulus trigger being the logic AND function of $SDO_{2,3}$.

A. Experiments With Anesthetized Rats

Microelectrodes were acutely implanted in two spatially separated forelimb motor areas of the rat's brain that are reciprocally connected with one another. Specifically, a micromachined silicon microelectrode with recording sites of iridium (NeuroNexus Technologies, Ann Arbor, MI) with impedance values of 2 to 3 MΩ was implanted in the rostral forelimb area (RFA), and a tungsten, matrix, stimulation electrode (FHC, Bowdoin, ME) with impedance value of 50 to 100 kΩ was implanted in the caudal forelimb area (CFA). Each electrode was externally interfaced with a single data channel of the recording front-end and stimulating back-end on the ASIC. A connection to the animal tail was tied to the system ground and used as a reference electrode for both recording and stimulation. In the first experiment, the CFA was stimulated at 2 Hz with a single monophasic current pulse [90 μA, 192 μs, see Fig. 6(a)], using an external trigger signal. Fig. 6(b) shows three traces of the recorded data from the RFA, depicting stimulus artifacts with duration of ∼4 ms and four neural spikes detected by the ASIC shortly after stimulation. Fig. 6(c) shows the raster plot and peristimulus histogram of the neural response to ICMS for a total of 315 ICMS pulses, depicting a clear increase in neural activity 7.5 ms after stimulation. This experiment demonstrates the system capability for simultaneous stimulation and recording the neural response to ICMS.

In a second acute experiment, neural activity was recorded on all four channels of the ASIC front-end to perform multichannel spike-triggered ICMS. If a spike event was accepted on any channel, the corresponding SDO was activated for 10 ms after a time delay of 5 ms. The decision circuitry was programmed to trigger ICMS whenever neural activity was simultaneously present on channels 2 and 3. Fig. 7 shows the simultaneously recorded data on each channel at the output of the digital HPF along with the corresponding SDO and the resulting stimulus trigger signal during a 300-ms time window. Two large stimulus artifacts were distinguishable on each channel as a result of spike-triggered stimulation, when simultaneous spike events (within a 10-ms window) occurred on channels 2 and 3. The data in both acute experiments were recorded via the wired link.

B. Experiments With Ambulatory Rats

Two micromachined silicon microelectrodes (NeuroNexus Technologies, Ann Arbor, MI) were chronically implanted in the RFA and second somatosensory area (SII) of the rat's brain for recording and stimulation, respectively, using standard neurosurgical techniques. The recording microelectrode had sixteen 413-μm^2 iridium sites uniformly placed along the length of its 3-mm silicon shank. The stimulation electrode had sixteen 1250-μm^2 sites uniformly placed along its 2-mm shank. The stimulation sites were also activated with iridium oxide (IrO) to further reduce the site impedance to ∼60–120 kΩ. A stainless steel threaded rod was mounted through an opening in the skull and affixed to it with acrylic. As shown in Fig. 8, the microdevice was mounted ∼1 cm above the rat's head and affixed to the skull using the threaded rod and nut, in such a way that the rat could not reach the microdevice. The threaded rod was also tied to the system ground and used as a reference electrode for both recording and stimulation.

Spontaneous neural activity was recorded on two of the four recording channels (Channels 3 and 4). The top two plots in Fig. 9 depict the data recorded at the output of the digital HPF

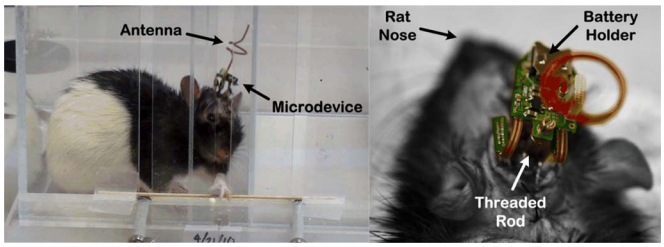

Fig. 8. (Left) Ambulatory rat instrumented with the microdevice inside a Plexiglas chamber for training. (Right) Close-up view of the microdevice on top of the rat's head.

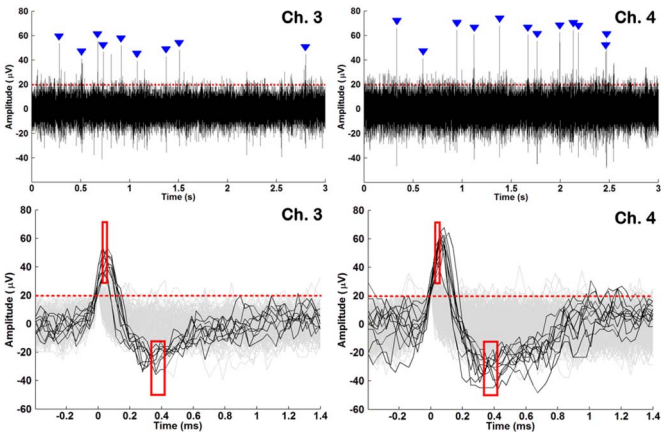

Fig. 9. (Top) 3-s window of neural activity recorded on channels 3 and 4 of the microdevice in an ambulatory rat. (Bottom) Operation of the time-amplitude window discriminator. Spike waveforms in dark gray (and with blue markers in top plot) were accepted for stimulus triggering, whereas those in light gray were rejected by the spike discriminator.

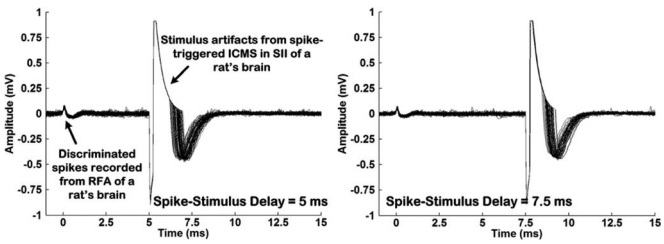

Fig. 10. Stimulation on the microelectrode implanted in the SII triggered by neural spikes discriminated on the electrode implanted in the RFA with spike-stimulus delays of 5 and 7.5 ms. The data were recorded wirelessly with the amplitude levels referred to the input.

within a 3-s window, and the bottom two plots depict the superimposed, time-aligned spike waveforms that crossed the user-positioned 20-μV threshold level (red dashed line). The accepted spikes (indicated with blue markers in top and as dark gray in bottom plots) also passed through the two time-amplitude window discriminators (solid red boxes), whereas the waveforms in light gray were rejected by the spike discriminator (i.e., not used for stimulus triggering).

The microdevice was programmed to trigger ICMS on all four stimulation channels using accepted spikes recorded on channel 4. Upon each trigger, the microdevice delivered a single monophasic current pulse (30 μA, 192 μs) with passive discharge to stimulate the target cortical tissue. The DSP operation

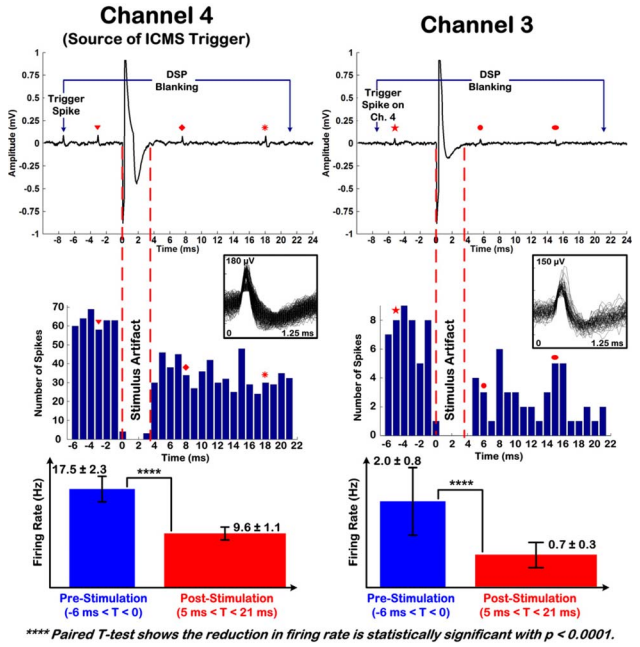

Fig. 11. Modulation of the neuronal firing rate due to ICMS triggered by neural spikes discriminated on channel 4. (Top) 34-ms window of recorded data on channels 3 and 4, showing a stimulus artifact and neural spikes. (Middle) Peristimulus histogram of neural activity (1-ms bins) during DSP blanking period. (Bottom) Mean neuronal firing rate pre- and poststimulation. Paired T-test showed the reduction in firing rate was statistically significant with $p < 0.0001$. Insets depict the time-aligned and superimposed neural spikes in each histogram, except for those at $t = 0$ (4 spikes on channel 4 and 1 spike on channel 3). The data were recorded via the wired link.

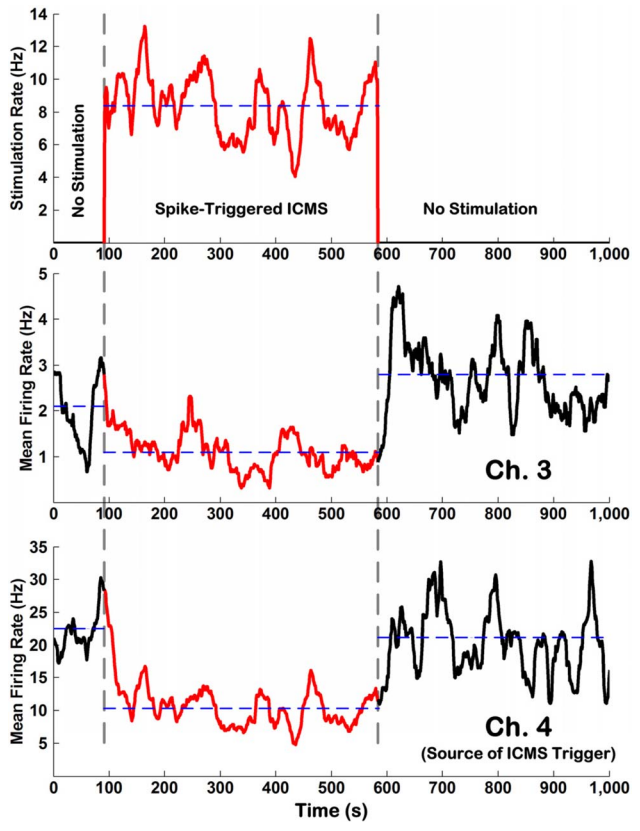

Fig. 12. Modulation of the neuronal firing rate due to ICMS triggered by neural spikes discriminated on channel 4 over a much longer time scale.

TABLE I
COMPARISON OF MICRODEVICE FUNCTIONALITY AND MEASURED PERFORMANCE

	This Work	[6]	[18]	[19]
Device Functionality	Activity-dependent ICMS	Activity-dependent ICMS	Neural recording	Neural recording
Type of Neural Recording	Extracellular action potentials	Extracellular action potentials	Extracellular action potentials / LFP	Extracellular action potentials / LFP
# of Recording Channels	4	1	1	32
Sampling Rate / Resolution	35.7 kS/s / 10 bits	11.7 kS/s / 8 bits	15.7 kS/s / 10 bits	30 kS/s / 12 bits
Type of Neural Stimulation	Monophasic w/ passive discharge	Biphasic	N/A	N/A
# of Stimulation Channels	4	1	N/A	N/A
Type of Neural Signal Processing	Spike discrimination w/ thresholding and two time-amplitude windows	Spike discrimination w/ thresholding and two time-amplitude windows	N/A	N/A
Communication Scheme	FSK @ ~433 MHz	Infrared (IR)	FSK @ ~900 MHz	FSK @ ~3.9 GHz
Data Rate	500 kb/s	57.6 kb/s	345.6 kb/s	24 Mb/s
Transmission Range	1 – 2 m	1 m	4 m	20 m
Total Dimensions	$3.6 \times 1.3 \times 0.6$ cm^3	$5.5 \times 5 \times 3$ cm^3	$3.8 \times 3.8 \times 5.1$ cm^3	$3.8 \times 3.8 \times 5.1$ cm^3
Total Weight w/ Battery	1.7 g	56 g	114 g	N/A
Type of Battery	1.55 V, 26 mAh silver-oxide (×1)	3.3 V, 2000 mAh Lithium (×1)	3.6 V, 1120 mAh Lithium (×1)	3.6 V, 1200 mAh Li-$SOCl_2$ (×2)
Power Consumption	0.42 mW	40 – 120 mW	63.2 mW	142 mW
Battery Lifetime	24 h	60 h	2.9 days	33 h
Experimental Paradigm	*In vivo* w/ ambulatory rats	*In vivo* w/ unrestrained primates	*In vivo* w/ freely moving primates	*In vivo* w/ freely moving primates
Publication Year	2011, TBME	2005, Neurosci. Methods	2009, TNSRE	2010, TBCAS

was also blanked for ~28.5 ms after each spike discrimination (i.e., neural spikes on channel 4 did not trigger ICMS during this period). Fig. 10 shows the superimposed spike waveforms and corresponding stimulus artifacts from single-pulse stimulation with spike-stimulus delays of 5 and 7.5 ms. The data were recorded wirelessly as the microdevice operated autonomously from a single 1.55-V battery.

The recorded data from channels 3 and 4 (corresponding to the spike-stimulus delay case of 7.5 ms) were further analyzed to investigate whether spike-triggered ICMS induced any electrophysiological change in the cortical circuitry. This was intended to show the physiological effect of the stimulating electrode beyond simply showing the stimulus artifact. The top left plot in Fig. 11 depicts a 34-ms window of the recorded data on channel 4, showing the trigger spike, the resulting stimulus artifact, and three other spikes that occurred during the DSP blanking period (indicated by red markers). The middle left plot depicts the peristimulus histogram (1-ms bins) during the DSP blanking period for 3600 trials. The trigger spikes occurred just prior to the start of the histogram. The histogram suggests that the neuronal firing rate after ICMS was lower than that prior to stimulation. A paired *T*-test also confirmed that the reduction of the neuronal firing rate after ICMS was statistically significant with $p < 0.0001$. The bottom left plot depicts the mean neuronal firing rate (±99% confidence interval) before and after ICMS on channel 4. The same effect was also observed on channel 3 as shown in the plots on the right, although generally fewer spikes were recorded on that channel throughout the experiment.

To determine whether the firing rate returned to baseline levels after the cessation of stimulation, we further examined the effect of spike-triggered ICMS over a much longer time scale, beginning ~90 s before stimulation, then during the 500-s stimulation period, and for ~410 s after stimulation (see Fig. 12.) The top plot depicts the measured stimulation rate versus time, whereas the middle and bottom plots depict the mean neuronal firing rate on channels 3 and 4, respectively. The data were smoothed by applying a moving average with a 25-s time window. The dashed lines show the average level for each section of the plot in time. Fig. 12 clearly shows that the neuronal firing rate not only decreases during spike-triggered ICMS, but also that it returns to the prestimulus level once ICMS is terminated.

Further, as expected, the stimulation rate is slightly below the neuronal firing rate on channel 4 during ICMS, because the spike events on channel 4 that occur during the DSP blanking period do not trigger stimulation. The reduction in spiking rate of channel 4 (and to a lesser extent, channel 3) is likely the result of activating horizontal connections that project from the point of stimulation to the recording site. These projections can innervate inhibitory interneurons that, when activated, would lead to a reduction of the activity of the recorded neurons [17].

IV. CONCLUSION

We presented data demonstrating the functionality of a microdevice for spike-triggered ICMS in an ambulatory rat. A previously developed multichannel ASIC for activity-dependent neurostimulation was custom assembled and packaged on a rigid-flex substrate, mounted on top of the rat's head, and interfaced with chronic silicon microelectrodes implanted in the rat's cerebral cortex. The microdevice successfully delivered electrical stimuli to the SII when triggered by neural activity discriminated from the RFA with a user-adjustable spike-stimulus time delay during autonomous operation with an onboard 1.55-V battery. The spike-triggered ICMS was further shown to be physiologically effective by modulating the neuronal firing

rate. Table I compares the microdevice functionality and measured performance with that of state-of-the-art in instrument development for awake, freely behaving animals [6], [18], [19]. The microdevice is currently being used to investigate the feasibility of guiding axonal sprouting and repairing interrupted cortical pathways directly within the brain post TBI by driving temporal coupling of activity between two distant brain regions [20].

ACKNOWLEDGMENT

The design, implementation, testing, and characterization of the microdevice were performed at Case Western Reserve University. The biological experiments were conducted at Kansas University Medical Center.

REFERENCES

[1] D. J. McFarland and J. R. Wolpaw, "Brain–computer interface operation of robotic and prosthetic devices," *Computer*, vol. 41, no. 10, pp. 52–56, Oct. 2008.

[2] M. Velliste, S. Perel, M. C. Spalding, A. S. Whitford, and A. B. Schwartz, "Cortical control of a prosthetic arm for self-feeding," *Nature*, vol. 453, pp. 1098–1101, Jun. 2008.

[3] L. R. Hochberg, M. D. Serruya, G. M. Friehs, J. A. Mukand, M. Saleh, A. H. Caplan, A. Branner, D. Chen, R. D. Penn, and J. P. Donoghue, "Neuronal ensemble control of prosthetic devices by a human with tetraplegia," *Nature*, vol. 442, pp. 164–171, Jul. 2006.

[4] J. D. Weiland and M. S. Humayun, "Intraocular retinal prosthesis," *IEEE Eng. Med. Biol. Mag.*, vol. 25, no. 5, pp. 60–66, Sep./Oct. 2006.

[5] J. P. Rauschecker and R. V. Shannon, "Sending sound to the brain," *Science*, vol. 295, no. 5557, pp. 1025–1029, Feb. 2002.

[6] J. Mavoori, A. Jackson, C. Diorio, and E. Fetz, "An autonomous implantable computer for neural recording and stimulation in unrestrained primates," *J. Neurosci. Methods*, vol. 148, pp. 71–77, 2005.

[7] A. Jackson, C. T. Moritz, J. Mavoori, T. H. Lucas, and E. E. Fetz, "The neurochip BCI: Towards a neural prosthesis for upper limb function," *IEEE Trans. Neural Syst. Rehabil. Eng.*, vol. 14, no. 2, pp. 187–190, Jun. 2006.

[8] C. T. Moritz, S. I. Perlmutter, and E. E. Fetz, "Direct control of paralyzed muscles by cortical neurons," *Nature*, vol. 456, pp. 639–643, 2008.

[9] A. Jackson, J. Mavoori, and E. E. Fetz, "Long-term motor cortex plasticity induced by an electronic neural implant," *Nature*, vol. 444, pp. 56–60, 2006.

[10] S. Venkatraman, K. Elkabany, J. D. Long, Y. Yao, and J. M. Carmena, "A system for neural recording and closed-loop intracortical microstimulation in awake rodents," *IEEE Trans. Biomed. Eng.*, vol. 56, no. 1, pp. 15–22, Jan. 2009.

[11] A. T. Avestruz, W. Santa, D. Carlson, R. Jensen, S. Stanslaski, A. Helfenstine, and T. Denison, "A 5 μW/channel spectral analysis IC for chronic bidirectional brain–machine interfaces," *IEEE J. Solid-State Circuits*, vol. 43, no. 12, pp. 3006–3024, Dec. 2008.

[12] T. Chen, K. Chen, Z. Yang, K. Cockerham, and W. Liu, "A biomedical multiprocessor SoC for closed-loop neuroprosthetic applications," in *Dig. Tech. Papers IEEE Int. Solid-State Circuits Conf.*, San Francisco, CA, Feb. 8–12, 2009, pp. 434–435.

[13] N. Dancause, S. Barbay, S. B. Frost, E. J. Plautz, D. Chen, E. V. Zoubina, A. M. Stowe, and R. J. Nudo, "Extensive cortical rewiring after brain injury," *J. Neurosci.*, vol. 25, no. 44, pp. 10167–10179, 2005.

[14] R. J. Nudo, "Mechanisms for recovery of motor function following cortical damage," *Curr. Opin. Neurobiol.*, vol. 16, pp. 1–7, 2006.

[15] M. Azin, D. J. Guggenmos, S. Barbay, R. J. Nudo, and P. Mohseni, "A battery-powered activity-dependent intracortical microstimulation IC for brain–machine–brain interface," *IEEE J. Solid-State Circuits*, vol. 46, no. 4, pp. 731–745, Apr. 2011.

[16] M. Nishibe, S. Barbay, D. Guggenmos, and R. J. Nudo, "Reorganization of motor cortex after controlled cortical impact in rats and implications for functional recovery," *J. Neurotrauma*, vol. 27, pp. 2221–2232, Dec. 2010.

[17] A. Keller and H. Asanuma, "Synaptic relationships involving local axon collaterals of pyramidal neurons in the cat motor cortex," *J. Comp. Neurol.*, vol. 336, pp. 229–242, 1993.

[18] C. A. Chestek, V. Gilja, P. Nuyujukian, R. J. Kier, F. Solzbacher, S. I. Ryu, R. R. Harrison, and K. V. Shenoy, "HermesC: Low-power wireless neural recording system for freely moving primates," *IEEE Trans. Neural Syst. Rehabil. Eng.*, vol. 17, no. 4, pp. 330–338, Aug. 2009.

[19] H. Miranda, V. Gilja, C. A. Chestek, K. V. Shenoy, and T. H. Meng, "HermesD: A high-rate long-range wireless transmission system for simultaneous multichannel neural recording applications," *IEEE Trans. Biomed. Circuits Syst.*, vol. 4, no. 3, pp. 181–191, Jun. 2010.

[20] M. Azin, D. J. Guggenmos, S. Barbay, R. J. Nudo, and P. Mohseni, "An integrated microsystem for neuroanatomical rewiring of cortical circuitry," in *Proc. 39th Neural Interfaces Conf.*, Long Beach, CA, Jun. 21–23, 2010, p. 124.

Meysam Azin (S'06) was born in 1980. He received the B.S. degree from the Amir Kabir University of Technology, Tehran, Iran, in 2002, the M.S. degree from the Sharif University of Technology, Tehran, in 2004, and the Ph.D. degree from Case Western Reserve University, Cleveland, OH, in 2011, all in electrical engineering.

His dissertation research was focused on developing ultralow-power, highly integrated biomedical systems for interfacing with the central nervous system. Upon graduation, he joined the West Wireless Health Institute, La Jolla, CA, where he is currently a Research Engineer. In 2004–2006, he was with KavoshCom Asia, a private R&D company in Tehran, where he was directing a design team to develop a low-cost WiFi IP phone. His research interests include analog and mixed-mode integrated circuits for advanced biomedical microsystems, low-power wireless sensors, and high-performance data converters.

David J. Guggenmos was born in 1983. He received the B.S. degree in psychology from Iowa State University, Ames, IA, in 2005. Since 2005, he has been working toward the Ph.D. degree at the University of Kansas Medical Center, Kansas City.

His research interests include motor cortical plasticity and the effects of electrical stimulation on neural tissue.

Scott Barbay was born in 1957. He received the B.S. and M.S. degrees in experimental psychology from the University of Louisiana, Lafayette, in 1980 and 1989, respectively, and the Ph.D. degree from Texas Christian University, Fort Worth, concentrating on behavioral neuroscience, in 1994. He has had postdoctoral training from the Laboratory of Systems Neuroscience, National Institute of Mental Health, Poolesville, MD, in 1994–1996 and at the Department of Neurobiology and Anatomy, University of Texas Health Science Center, Houston, in 1996–1997.

He is currently a Senior Scientist in the Cortical Plasticity Laboratory, Department of Molecular and Integrative Physiology and Landon Center on Aging, University of Kansas Medical Center, Kansas City. His research interests include translational models of stroke recovery that emphasize neurophysiological and neuroanatomical reorganization within the cerebral cortex associated with recovery of motor function after stroke.

Dr. Barbay is a member of the Society for Neuroscience and the Association for Psychological Science.

Randolph J. Nudo was born in Uniontown, PA, in 1953. He received the degree in electrical engineering from the University of Notre Dame, South Bend, IN, the B.S. degree in psychology from Pennsylvania State University, University Park, PA, in 1977, and the M.S. and Ph.D. degrees in psychology from Florida State University, Tallahassee, FL, in 1980 and 1985, respectively. He completed the postdoctoral fellowship in physiology at the University of California, San Francisco, in 1987.

He joined the faculty of the University of Texas Health Science Center, Houston, as a tenure-track Assistant Professor in 1988, and was promoted to an Associate Professor with tenure in 1996. Since 1997, he has been with the faculty of the University of Kansas Medical Center, Kansas City, now holding the titles of a Professor of molecular and integrative physiology, a Marion Merrell Dow Distinguished Professor in aging, and the Director of the Landon Center on aging. He is the author or coauthor of papers published in numerous high-profile journals in the field of neuroscience, including *Science, The Journal of Neuroscience*, *Journal of Neurophysiology, Cerebral Cortex, and Nature Medicine*. His research interests focus on translating basic science research into more effective clinical interventions for neurological disorders that accompany aging. He is recognized internationally for his work on the effects of rehabilitative training on functional plasticity after stroke. His research activities are currently funded by the National Institutes of Health, U.S. Army, and the American Heart Association. He is on the editorial boards of *Neurorehabilitation and Neural Repair, Restorative Neurology and Neuroscience, and Neuroscience and Biobehavioral Reviews*. He is also deputy editor of Brain Stimulation, Basic, Translational and Clinical Research in Neuromodulation.

Dr. Nudo is a member of the board of directors of the American Society of Neurorehabilitation. He received the prestigious Javits Investigator Award in neuroscience, in 2007.

Pedram Mohseni (S'94–M'05–SM'11) was born in 1974. He received the B.S. degree in electrical engineering from the Sharif University of Technology, Tehran, Iran, in 1996, and the M.S. and Ph.D. degrees in electrical engineering from the University of Michigan, Ann Arbor, in 1999 and 2005, respectively.

He joined the Faculty of the Department of Electrical Engineering and Computer Science (EECS), Case Western Reserve University, Cleveland, OH, as a tenure-track Assistant Professor in August 2005 with a secondary appointment in the Department of Biomedical Engineering starting in 2009. He was promoted to the rank of Associate Professor with the Award of Tenure in 2011. He is the author or coauthor of numerous papers published in refereed IEEE journals and conferences, and has served as a technical reviewer for a number of the IEEE publications. His research interests include analog/mixed-signal/RF integrated circuits and microsystems for neural engineering, wireless sensing/actuating systems for brain–machine interfaces, biomedical microtelemetry, and assembly/packaging of biomicrosystems.

Dr. Mohseni is a member of the IEEE Solid-State Circuits, Circuits & Systems, and Engineering in Medicine and Biology Societies. He is currently an Associate Editor for the IEEE TRANSACTIONS ON CIRCUITS AND SYSTEMS-PART II and IEEE TRANSACTIONS ON BIOMEDICAL CIRCUITS AND SYSTEMS, and also serves on the Analog Signal Processing and Biomedical Circuits and Systems Technical Committees of the IEEE Circuits & Systems Society. He is a recipient of the 2008 EECS Faculty Research Award for Exceptional Achievement, 2009 National Science Foundation CAREER Award, and 2011 Case School of Engineering Research Award.